JOURNAL OF VIROLOGY, Dec. 2005, p. 15405–15416 Vol. 79, No. 24
0022-538X/05/$08.00+0 doi:10.1128/JVI.79.24.15405–15416.2005

Overexpression of Tumor Necrosis Factor Alpha by a Recombinant Rabies Virus Attenuates Replication in Neurons and Prevents Lethal Infection in Mice

Milosz Faber,[1]† Michael Bette,[2]† Mirjam A. R. Preuss,[2,3] Rojjanaporn Pulmanausahakul,[1] Jennifer Rehnelt,[2] Matthias J. Schnell,[3] Bernhard Dietzschold,[1] and Eberhard Weihe[2]*

Department of Microbiology and Immunology, Center for Neurovirology,[1] and Department of Biochemistry and Molecular Pharmacology,[3] Thomas Jefferson University, Philadelphia, Pennsylvania, and Department of Molecular Neuroscience, Institute of Anatomy and Cell Biology, Philipps University Marburg, Marburg, Germany[2]

Received 7 June 2005/Accepted 19 September 2005

The effect of tumor necrosis factor alpha (TNF-α) on rabies virus (RV) infection of the mouse central nervous system (CNS) was studied, using recombinant RV engineered to express either soluble TNF-α [SPBN-TNF-α(+)] or insoluble membrane-bound TNF-α [SPBN-TNF-α(MEM)]. Growth curves derived from infections of mouse neuroblastoma NA cells revealed significantly less spread and production of SPBN-TNF-α(+) than of SPBN-TNF-α(MEM) or SPBN-TNF-α(−), which carries an inactivated TNF-α gene. The expression of soluble or membrane-bound TNF-α was not associated with increased cell death or induction of alpha/beta interferons. Brains of mice infected intranasally with SPBN-TNF-α(+) showed significantly less virus spread than did mouse brains after SPBN-TNF-α(−) infection, and none of the SPBN-TNF-α(+)-infected mice succumbed to RV infection, whereas 80% of SPBN-TNF-α(−)-infected mice died. Reduced virus spread in SPBN-TNF-α(+)-infected mouse brains was paralleled by enhanced CNS inflammation, including T-cell infiltration and microglial activation. These data suggest that TNF-α exerts its protective activity in the brain directly through an as yet unknown antiviral mechanism and indirectly through the induction of inflammatory processes in the CNS.

Rabies is a central nervous system (CNS) disease that is almost invariably fatal. Neuroinvasiveness, neurotropism, and impairment of neuronal functions are the major defining characteristics of a classical rabies virus (RV) infection.

Virus-neutralizing antibodies, adaptive T-cell-mediated responses, and innate responses mediated by nonspecific cells such as macrophages all play a role in the immune defense against rabies (9, 13). One of the most important cytokines of adaptive and innate immunity is tumor necrosis factor alpha (TNF-α), a proinflammatory cytokine produced by T cells and cells of the monocyte/macrophage lineage, including microglial cells (3, 4). TNF-α has direct cytotoxic and pleiotropic immunomodulatory/neurotrophic effects (39). TNF-α is produced as a 26-kDa transmembrane protein, from which the mature soluble 17-kDa form is cleaved by matrix metalloproteinase enzymes (18). TNF-α signals through TNF receptor 1 (TNFR1), the primary receptor for soluble TNF-α, and TNF receptor 2 (TNFR2), the main receptor for membrane-bound TNF-α (38). The homotrimer of the 17-kDa secreted molecule is the major biologically active form of TNF (33). Soluble TNF-α mediates apoptosis, mainly through engagement with TNFR1, and promotes inflammation through the activation of macrophages and NK cells and the induction of other cytokines and adhesion molecules (25, 36). The 26-kDa membrane-bound form of TNF-α is also biologically active, inducing apoptosis, cytokine production, and cell proliferation in appropriate cell lines as efficiently as soluble TNF-α by acting through the TNFR1 and/or TNFR2 receptor; however, the membrane-bound form of TNF-α proved to be less active than soluble TNF-α in cytotoxic assays (10).

TNF-α plays an important role in bacterial and viral infections (6), inducing the expression of alpha/beta interferons (IFN-α/β) (16, 21) and exerting a strong direct antiviral activity against avian, swine, and human influenza viruses with a potency greater than that of interferons (32). The periodic administration of TNF-α to animals infected with encephalomyocarditis virus reduced viral titers in the brain, decreased the degree of clinical paralysis, and lessened the severity of inflammatory lesions in the brain (34). Both TNFR1 and TNFR2 are involved in the antiviral activity of TNF (29). It has been suggested that TNFR1 plays a role in the disease process caused by RV infection of the eyes and the brain (7, 8). In all cases, it remains unclear whether TNF-α-mediated immune responses during viral infection are protective, pathogenic, or both (27).

For this study, we tested whether TNF-α contributes to protection against lethal RV infection through a mechanism that inhibits virus replication, stimulates inflammatory responses in the brain, or both. We used recombinant RV to deliver TNF-α noninvasively (intranasally) to the brains of mice.

MATERIALS AND METHODS

Viruses, viral antigens, and cell lines. The recombinant RV vector SPBN was generated from an SAD B19 cDNA clone as described previously (22, 31).

* Corresponding author. Mailing address: Department of Molecular Neuroscience, Institute of Anatomy and Cell Biology, Philipps University Marburg, Robert-Koch Str. 8, D-35037 Marburg, Germany. Phone: 49-6421-2866247. Fax: 49-6421-2868965. E-mail: weihe@staff.uni-marburg.de.

† Both authors contributed equally to the study.

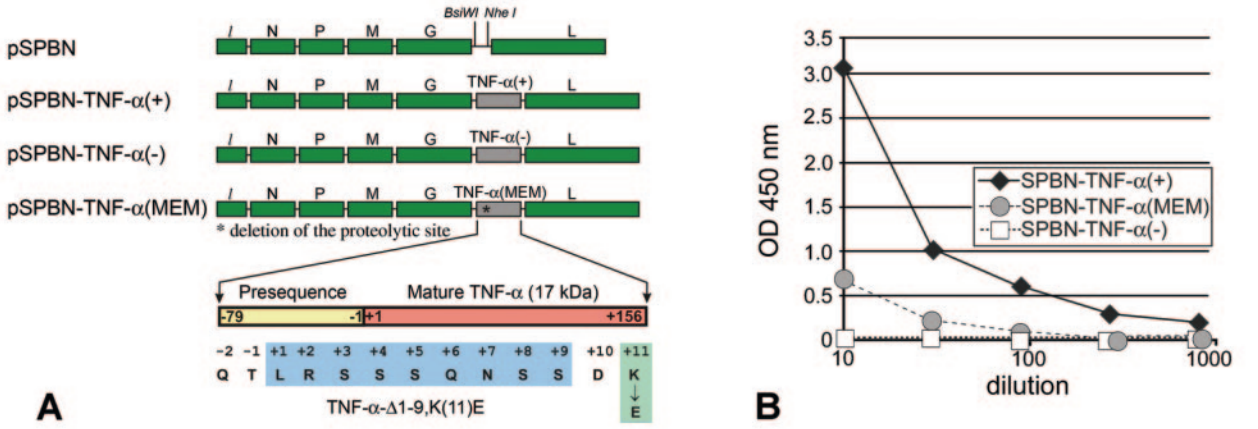

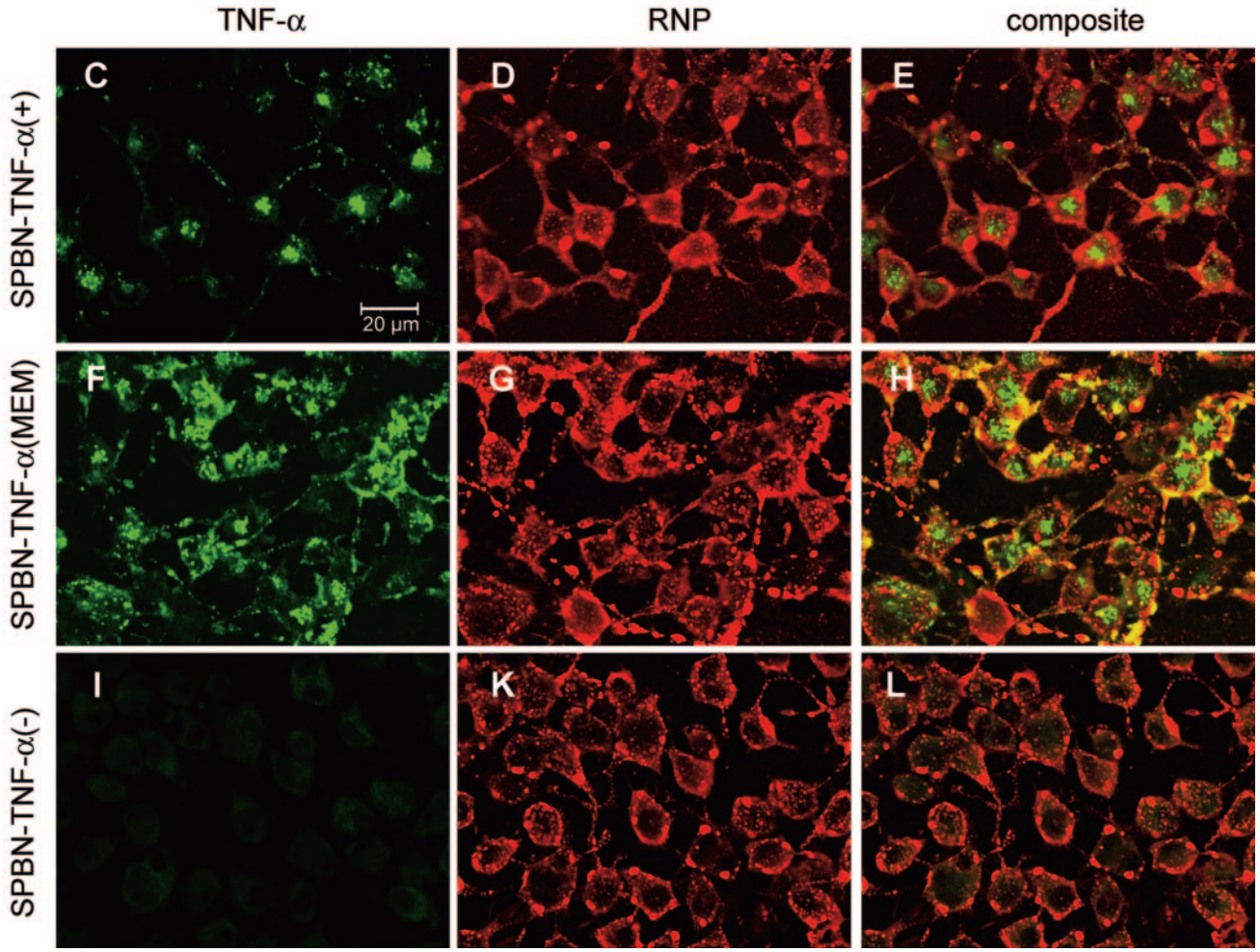

FIG. 1. Expression of TNF-α by recombinant RV. (A) Schematic of RV–TNF-α recombinant constructs. The pSPBN vector was derived from SN by removing the Ψ gene and introducing BsiWI and NheI sites between the G and L genes. Mouse TNF-α cDNA was amplified by PCR, with the introduction of BsiWI and NheI sites, and was ligated into pSPBN, resulting in pSPBN-TNF-α(+). In pSPBN-TNF-α(MEM), the proteolytic cleavage site of TNF-α was removed by deleting the coding sequence for the first nine amino acids of soluble TNF-α and exchanging the lysine at position 11 with glutamic acid, as described in Materials and Methods. To construct pSPBN-TNF-α(−), the first seven ATG codons of the TNF-α gene were mutated. (B) TNF-α production in BSR cells. BSR cells were infected with SPBN-TNF-α(−), SPBN-TNF-α(MEM), or SPBN-TNF-α(+) at an MOI of 0.1 and incubated at 37°C. TNF-α secreted into the tissue culture supernatants of infected BSR cells was measured at 24 h p.i., using ELISA. OD, optical density. (C to L) Confocal double-immunofluorescence microscopy of TNF-α (green, panels C, F, and I) and rabies ribonucleocapsid (RNP) (red, panels D, G, and K) in NA cells infected with SPBN-TNF-α(+), SPBN-TNF-α(MEM), or SPBN-TNF-α(−). Panels E, H, and L show the composites of TNF-α and RNP double immunofluorescence. Note that TNF-α is absent only in NA cells infected with SPBN-TNF-α(−) (panels I and L).

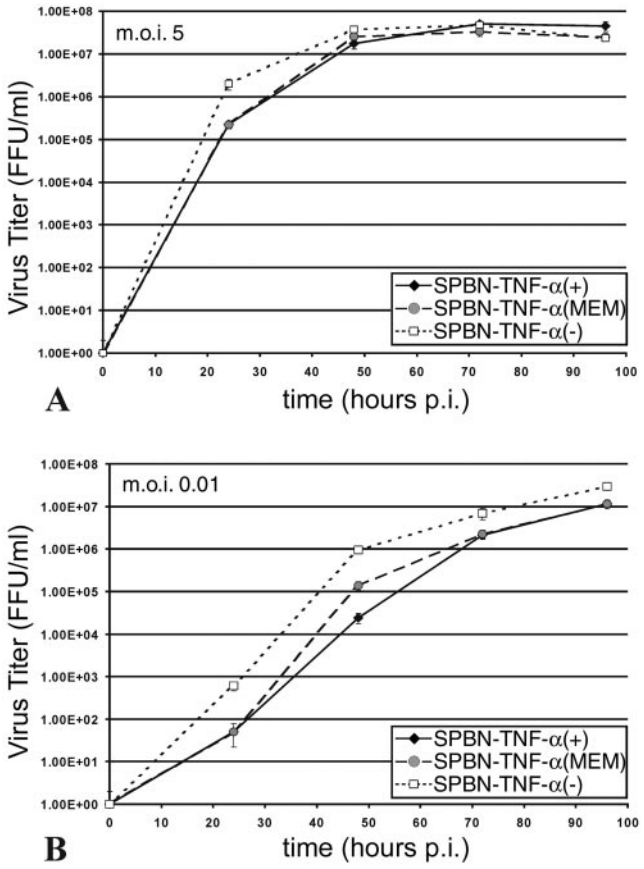

FIG. 2. Growth of TNF-α-expressing recombinant RV in NA cells. NA cells were infected with SPBN-TNF-α(−), SPBN-TNF-α(MEM), or SPBN-TNF-α(+) at an MOI of 5 (A) or 0.01 (B) and incubated at 34°C. At the indicated times p.i., viruses were harvested and titrated. All titrations were carried out in quadruplicate, and titers are expressed as mean values ± SEM. The statistical significance among titers produced by the different recombinant RVs was determined using one-way ANOVA with the Newman-Keuls multiple comparison test.

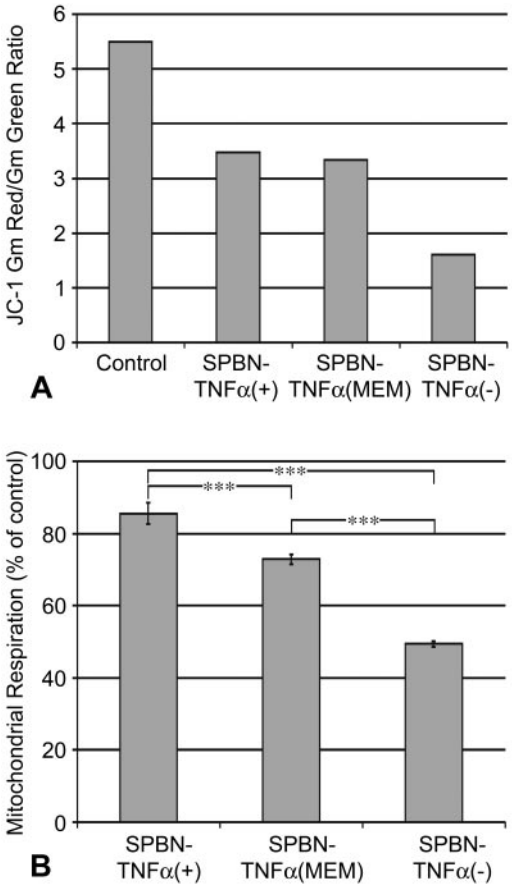

FIG. 3. Effect of TNF-α expressed by recombinant RV infection on mitochondrial membrane potential (A) and mitochondrial respiration (B) in mouse neuroblastoma NA cells. (A) Flow cytometry of noninfected (control) and infected NA cells labeled with JC-1. The mitochondrial membrane potential is expressed as the ratio of the geometric means (Gm) of red (JC-1 aggregates) and green (JC-1 monomers) fluorescence intensities. (B) Mitochondrial respiration in NA cells infected with recombinant RV was determined using the MTT assay described in Materials and Methods. Data are expressed as mean values ± SEM; asterisks indicate significant differences (***, $P < 0.001$) between experimental groups. Statistical significance was determined using one-way ANOVA with the Newman-Keuls multiple comparison test.

Neuroblastoma NA cells of A/J mouse origin were grown at 34°C in RPMI 1640 medium supplemented with 10% fetal bovine serum (FBS). BSR cells were grown at 34°C in Dulbecco's modified Eagle's medium supplemented with 10% FBS.

Construction of recombinant RV–TNF-α cDNA clones. Total cellular RNA was extracted from mouse brains, using the Ultraspec RNA isolation system (Biotecx Laboratories, Houston, TX), and reverse transcribed into cDNAs using avian myeloblastosis virus reverse transcriptase and an oligo(dT) primer (Promega, Madison, WI). Mouse TNF-α cDNA was amplified using Expand Hi-Fi *Taq* polymerase (Roche Applied Science, Indianapolis, IN) and the gene-specific primers TNF-1(+) (5′-AAACGTACG**ATG**AGCACAGAAAGCATGATC-3′ [a BsiWI site is underlined, and the start codon is shown in bold]) and TNF-2(−) (5′-AAAGCTAGC**TCA**CAGAGCAATGACTCCAAAG-3′ [an NheI site is underlined, and the stop codon is shown in bold]) to introduce BsiWI and NheI recognition sites before and after the TNF-α coding region. The PCR product was digested with BsiWI and NheI (New England Biolabs, Beverly, MA) and ligated into RV vector pSPBN that had been previously digested with BsiWI and NheI. The resulting plasmid was designated pSPBN-TNF-α(+) (Fig. 1A).

To construct a recombinant RV expressing insoluble, membrane-bound TNF-α, the proteolytic cleavage site in TNF-α was deleted (10). Briefly, the TNF-α fragment was amplified using Vent polymerase (New England Biolabs, Beverly, MA) and primers TNF-3(+) (5′-CCG*GAATTC*CGTACGAAG**ATG**AGCACAGAAAGCATGATCCGCGAC-3′ [an EcoRI site is shown in italics, a BsiWI site is underlined, and the start codon is shown in bold]) and TNF-5(−) (5′-TACCG*CTCGAG*CGGCGGCTAGCCGT**TCA**CAGAGCAATGACTCCAA-3′ [an XhoI site is shown in italics, an NheI site is underlined, and the stop codon is shown in bold]). The resulting PCR product was digested with EcoRI and XhoI and ligated into pCR2.1 (Invitrogen, Carlsbad, CA) that had been previously digested with the same restriction enzymes. Deletion of the 9-amino-acid coding sequence and site-directed mutagenesis of the 11th amino acid (Fig. 1A) were performed by a single PCR using an ExSite PCR-based site-directed mutagenesis kit (Stratagene, La Jolla, CA) with primers TNF-10(+) (5′-GAC**G AA**CCTGTAGCCCACGTCGTAGCAAACCACCAA-3′ [the GAA codon in bold represents the mutagenized amino acid]) and TNF-11(−) [5′-(P)TGTGA GGGTCTGGGCCATAGAACTGATGAGAGGGAG-3′] according to the manufacturer's recommendations. The PCR product was digested with BsiWI and NheI, and the modified TNF-α fragment was cloned into the pSPBN vector as described above. The resulting plasmid was designated pSPBN-TNF-α(MEM) (Fig. 1A).

To construct an RV control vector that does not express TNF-α, all ATG codons within the first 200 bases of the TNF-α gene were mutated into stop codons (TGA or TAG). The DNA fragment containing the TNF-α gene was amplified using primers TNF-4(+) (5′-CCG*GAATTC*CGTACGAAG**TGA**AGC

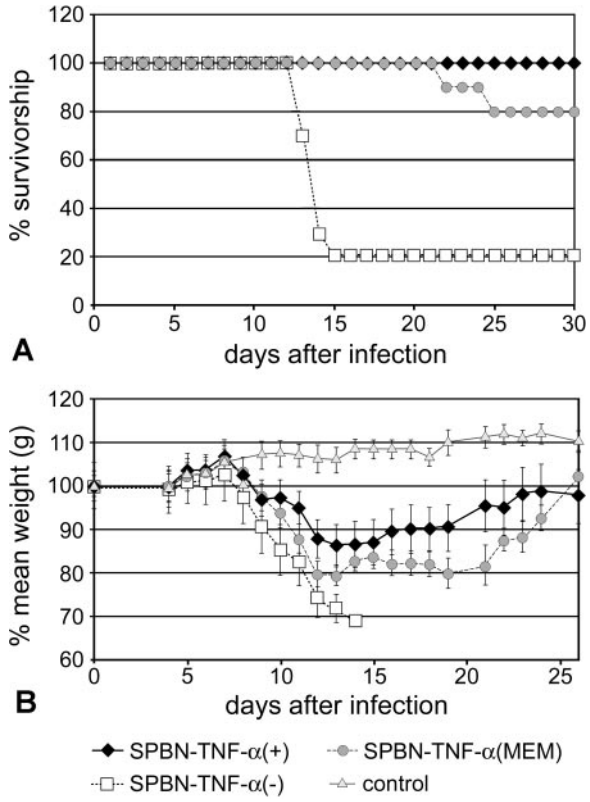

FIG. 4. Effect of intranasal infection with TNF-α-expressing recombinant RV on survival (A) and body weight (B) of TNF-α KO mice. Mice were infected i.n. with 10^5 FFU of SPBN-TNF-α(−), SPBN-TNF-α(+), or SPBN-TNF-α(MEM) or with saline (control). Mortality and body weight were recorded daily.

ACAGAAAGC**TGA**ATCCGCGAC-3′ [an EcoRI site is shown in italics, a BsiWI site is underlined, and the first two modified stop codons are shown in bold]) and TNF5(−) and cloned into pCR2.1 as described above; the remaining ATG codons were mutagenized in two subsequent steps using an ExSite PCR-based site-directed mutagenesis kit as described above, with the following primers: (i) TNF-6(+) (5′-**TGA**GGGGGCTTCCAGAACTCCAGGCGGTGCC**TT GA**TCTCAGCCT-3′) and TNF-7(−) [5′-(P)CTTTTGGGGGAGTGCCTCTTC TGCCAGTTCCACGTCGCGGAT-3′] and (ii) TNF-8(−) (5′-**TAG**GCCTCCC TCTCATCAGTTCT**TAG**GCCCAGACCCTCCAC-3′) and TNF-9(−) [5′-(P)T TGGGAACTTCT**CTA**CCCTTTGGGGACCGATCACCCCGAAGT-3′]. The DNA fragment containing the inactivated TNF-α gene was cloned into pSPBN as described above, and the final product was designated pSPBN-TNF-α(−) (Fig. 1A).

Sequences of all TNF-α DNA fragments were confirmed by restriction analysis and DNA sequencing. Recombinant RVs were rescued as described previously (22, 31). Briefly, BSR-T7 cells were transfected using a calcium phosphate transfection kit (Stratagene, La Jolla, CA) with 5.0 μg of pSPBN-TNF-α(+), pSPBN-TNF-α(MEM), or pSPBN-TNF-α(−), 5.0 μg of pTIT-N, 2.5 μg of pTIT-P, 2.5 μg of pTIT-L, and 2.0 μg of pTIT-G. After a 3-day incubation, supernatants were transferred onto BSR cells, and incubation was continued for 3 days at 37°C. Cells were examined for the presence of rescued virus by immunostaining with a fluorescein isothiocyanate-labeled antibody against the RV N protein (Centocor, Malvern, PA).

The correct nucleotide sequences of the inserted genes were confirmed by reverse transcription-PCR (RT-PCR) analysis and DNA sequencing.

Virus infectivity assay. Virus titers were determined using the fluorescence focus test as described previously (23). Briefly, NA cells grown in 96-well plates were infected with 100 μl/well of serial 10-fold virus dilutions in RPMI medium containing 0.2% bovine serum albumin (BSA) and incubated at 34°C for 48 h. After incubation, the culture supernatant was removed, and after fixation with ice-cold acetone, the cells were stained with fluorescein isothiocyanate-labeled antirabies antibodies (Centocor, Malvern, PA). Fluorescent foci were counted using a fluorescence microscope, and virus titers were calculated from the numbers of foci detected in wells infected with the highest virus dilution. All titrations were carried out in quadruplicate, and titers were expressed as mean values ± standard errors of the means (SEM). The statistical significance among titers produced by the different recombinant RVs was determined using one-way analysis of variance (ANOVA) with the Newman-Keuls multiple comparison test.

Analysis of TNF-α production by ELISA. BSR cells were infected with SPBN-TNF-α(+), SPBN-TNF-α(MEM), or SPBN-TNF-α(−) at a multiplicity of infection (MOI) of 0.1. At 24 h postinfection (p.i.), the amount of TNF-α secreted into the tissue culture supernatant was measured using a commercial TNF-α enzyme-linked immunosorbent assay (ELISA) kit (Quantikine M; R&D Systems, Minneapolis, MN).

Cell viability assay. Cell viability was assessed based on mitochondrial respiration (37), as indicated by the mitochondrion-dependent reduction of MTT (3-2,5-diphenyltetrazolium bromide; Sigma, St. Louis, MO). At 48 h p.i., NA cells were incubated with 0.2 mg of MTT/ml for 1 h at 37°C and lysed with dimethyl sulfoxide, and the reduction of MTT to formazan was quantitated using a microplate reader to measure the optical density at 550 nm.

Mitochondrial membrane potential assay. The loss of mitochondrial membrane potential of NA cells was determined by measuring the green and red fluorescence intensities with a JC-1 assay kit (Biotium, Hayward, CA). In non-apoptotic cells, JC-1 (5,5′,6,6′-tetrachloro-1,1′,3,3′tetraethylbenzimidazolylcarbocyanine) exists as a monomer in the cytosol (green fluorescence) and also accumulates as aggregates in mitochondria (red signal). In apoptotic cells, the mitochondrial membrane potential collapses and JC-1 cannot accumulate within the mitochondria. The NA cells were infected with recombinant RVs at an MOI of 5 or mock infected, incubated at 37°C for 48 h, and assayed according to the manufacturer's recommendations. Cells were then analyzed by flow cytometry (FACSCalibur; Beckton Dickinson, San Jose, CA). Data were expressed as mean values ± SEM. Significant differences were determined using one-way ANOVA with the Newman-Keuls multiple comparison test.

Treatment of NA cells with recombinant murine TNF-α. NA cells seeded at 5×10^4 cells/well of a 96-well plate were stimulated with recombinant murine TNF-α (Boehringer-Mannheim, Mannheim, Germany) at 50 pg/ml in RPMI 1640 medium supplemented with 10% FBS. The biological activity of the recombinant murine TNF-α was assessed based on its cytotoxic effect on actinomycin D-pretreated WEHI-164 cells as described previously (4). Stimulated NA cells were harvested after 48 h and washed in phosphate-buffered saline (PBS), and RNAs were isolated for RT-PCR analysis.

RT-PCR analysis. Total RNA was isolated from cultured NA cells, using TRIzol, and reverse transcribed with Superscript II RNase H^- reverse transcriptase (both from Invitrogen, Karlsruhe, Germany), and PCRs were performed using PCR Supermix (Life Technologies, Paisley, United Kingdom). The following primers were used: TNFR1 forward primer, 5′-GTGCCTACCTCCTCCGC TT-3′; TNFR1 lower primer, 5′-CAGCATACAGAATCGCAAGGTC-3′; TNFR2 upper primer, 5′-GCAACAAGACCTCGGACAC-3′; TNFR2 lower primer, 5′-GGCAGGAGGGCTTCTTTTTC-3′; alpha interferon 2 (IFN-α2) reverse primer, 5′-CAACCTCTGCAAGACCCAC-3′; IFN-α2 lower primer, 5′-G TCTCACACTCACTCCTTCTCTTC-3′; IFN-β upper primer, 5′-CACCAGCC TGGCTTCCATCATG-3′; IFN-β lower primer, 5′-TTCACTACCAGTCCCAG AGTCCGC-3′; glyceraldehyde-3-phosphate dehydrogenase upper primer, 5′-ACC CAGAAGACTGTGGATGG-3′; and glyceraldehyde-3-phosphate dehydrogenase lower primer, 5′-GGTCCTCAGTGTAGCCCAAG-3′.

Pathogenicity assay with mice. Groups of 10 6-week-old female Swiss Webster mice (Taconic Farms, Germantown, NY) or TNF-α knockout (KO) mice (B6 [129S6-Tnf^{tm1Gkl}/J]; Jackson Laboratory, Bar Harbor, ME) were infected intranasally (i.n.) under anesthesia with 10 μl of (PBS) containing 10^5 focus-forming units (FFU) of recombinant virus. Mice were monitored for the appearance of clinical signs of rabies and weighed daily.

All animal experiments were performed under Institutional Animal Care and Use Committee-approved protocols (animal welfare assurance no. A3085-01).

VNA assay. About 100 μl of blood was collected from the retro-orbital sinuses of mice under isoflurane inhalation anesthesia, and the sera were tested for the presence of virus-neutralizing antibodies (VNA) using the rapid fluorescence inhibition test (41). The neutralization titer, defined as the inverse of the highest serum dilution that neutralized 50% of the challenge virus, was normalized to international units using the World Health Organization anti-RV antibody standard. Geometric mean titers were calculated from individual titers of 10 mice that received identical concentrations of the same virus.

Immunohistochemical analysis. At different times after infection, mice were anesthetized and perfused transcardially with PBS containing procaine-HCl (5

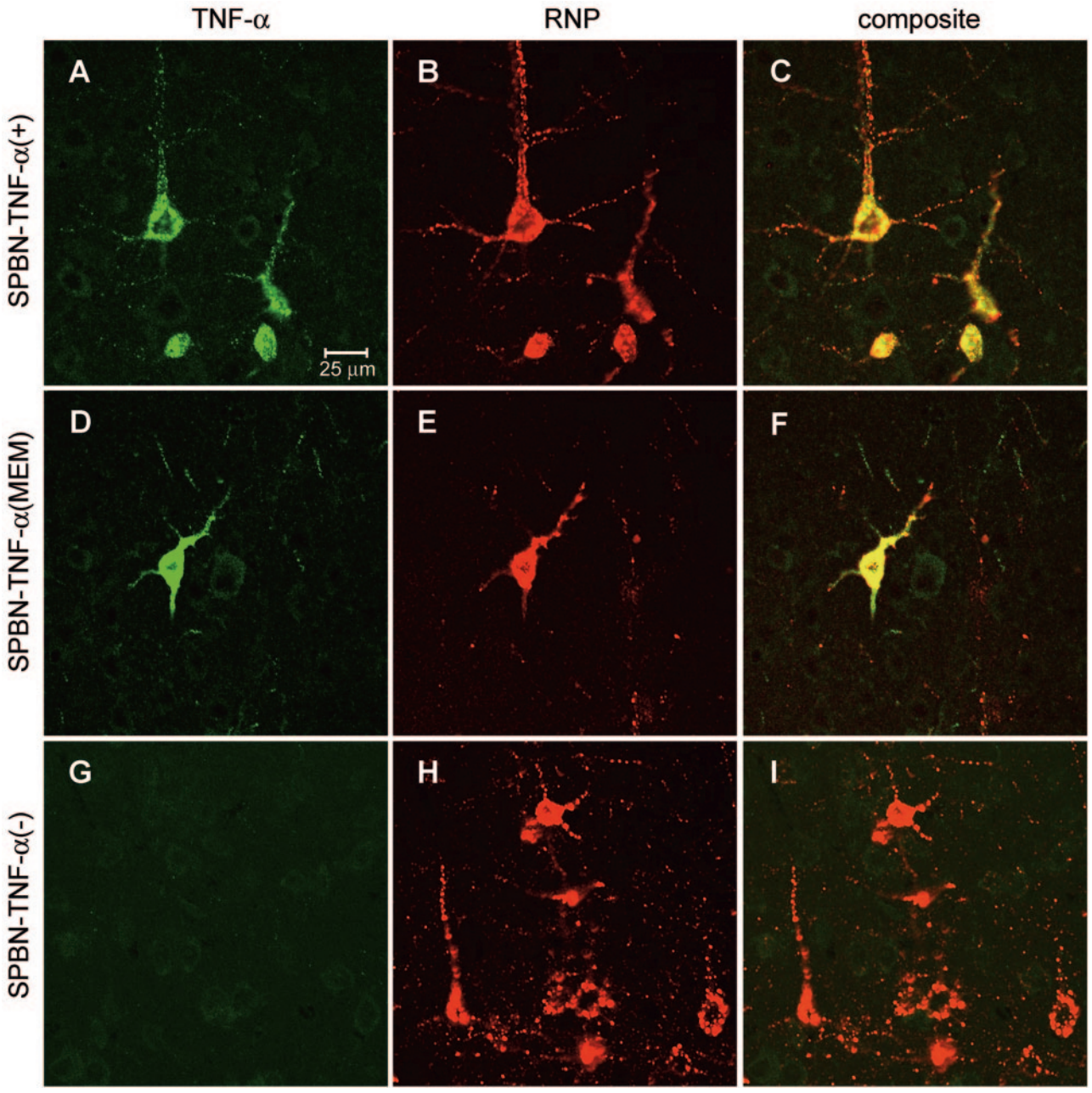

FIG. 5. Expression of TNF-α (green) in cerebral neurons infected with SPBN-TNF-α(+) (A to C) or SPBN-TNF-α(MEM) (D to F), but not in SPBN-TNF-α(−)-infected neurons (G to I), on day 10 p.i. in the cortexes of TNF-α KO mice. High-power double-immunofluorescence laser scanning microscopic images of TNF-α (green) and rabies ribonucleocapsid (RNP, red) expression are shown.

g/liter) and heparin (20,000 IU/liter) followed by Bouin-Hollande fixation solution (15). Brains were removed and postfixed for 24 h in the same fixative. After dehydration in a graded series of 2-propanol, tissues were embedded in Paraplast Plus (Merck, Darmstadt, Germany) and cut into 7-μm-thick coronal sections. Histological analysis was performed on coronal sections through the hippocampus. NA cells were fixed with 4% paraformaldehyde for 1 h and washed in 50 mM PBS several times before immunocytochemical analysis. For optimal antigen retrieval, brain sections and fixed cells were incubated in 10 mM sodium citrate buffer, pH 6.0, for 15 min at 95°C and blocked by successive 30-min incubations in BSA and avidin-biotin blocking solution (Vectastain Elite ABC kit; Vector Laboratories, Burlingame, CA) before the incubation of primary antisera.

For immunohistochemical analysis, adjacent brain sections were incubated with the following antibodies: (i) a polyclonal rabbit antibody raised against RV ribonucleoprotein (RNP) (28), diluted 1:3,000; (ii) a polyclonal rabbit antiserum against CD3 (MCA1477; Serotec, Oxford, United Kingdom) to localize T cells; and (iii) a polyclonal antiserum against ionized binding calcium adapter molecule 1 (Iba1) (Wako Pure Chemical Industries, Richmond, Virginia), diluted 1:3,000, to detect macrophages/microglial cells (11). Primary antibodies were applied in 1% BSA-PBS, and incubation was carried out overnight at 16°C followed by 2 h at 37°C. For bright-field analysis, immunoreactions were detected with species-specific biotinylated secondary antibodies (Dianova, Hamburg, Germany) by the Vectastain ABC method (Vectastain Elite ABC kit; Vector Laboratories, Burlingame, CA), including ammonium nickel sulfate-enhanced 3′,3-diaminobenzidine (DAB; Sigma, Deisenhofen, Germany) reactions.

For confocal double-immunofluorescence microscopy, the primary antiserum against RNP (diluted 1:300) and polyclonal goat antibodies that recognize mu-

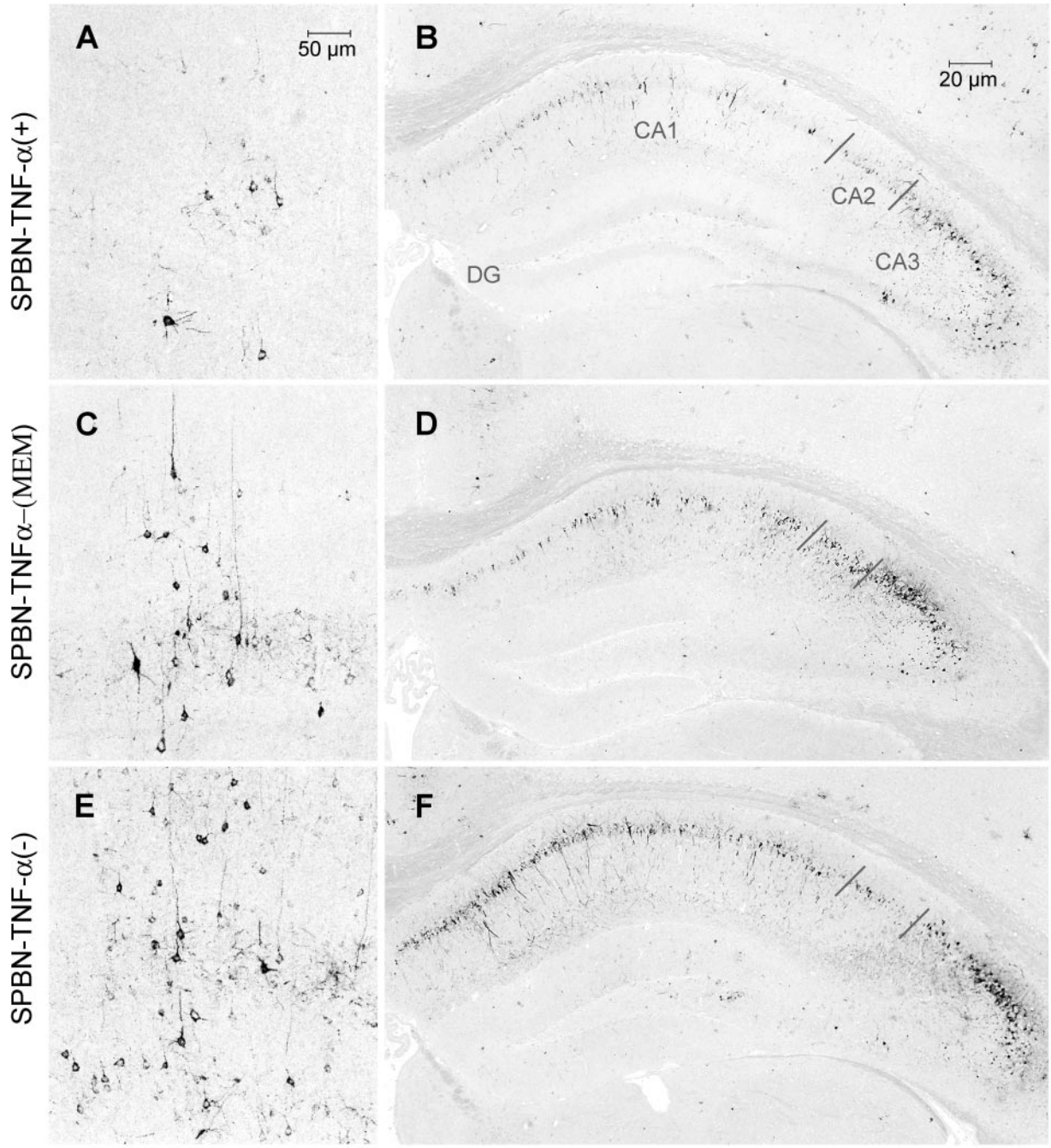

FIG. 6. Detection of RV-infected neurons in the brain. The images show the presence of rabies virus RNP in neurons of the cortexes (A, C, E) and the CA1-to-CA3 region of the hippocampal formations (B, D, F) of TNF-α KO mice on day 10 after infection with SPBN-TNF-α(+), SPBN-TNF-α(MEM), or SPBN-TNF-α(−). Bright-field microscopy of immunostained brain sections is shown. DG, dentate gyrus; CA, CA region of hippocampus. Quantitation of rabies virus-infected neurons (RNP) in the cerebral cortexes (G) and the CA1-to-CA3 region of the hippocampal formations (H) of TNF-α KO mice infected with SPBN-TNF-α(+), SPBN-TNF-α(MEM), or SPBN-TNF-α(−) was done at 10 days p.i. Data are expressed as mean values ± SEM; asterisks indicate significant differences (***, $P < 0.001$) between experimental groups, as calculated by ANOVA.

rine TNF-α (sc-1350, diluted 1:500 [Santa Cruz Biotechnology, Santa Cruz, CA], and PAK-mTNF-α-g50, diluted 1:100 [Strathmann Biotech AG, Hamburg, Germany]) (17) were coapplied to identical brain sections and cultured NA cells. Immunoreactions were visualized with species-specific secondary antibodies labeled with Alexa fluor 488 or Alexa fluor 647 (diluted 1:200; both from MoBiTec, Göttingen, Germany) and with species-specific biotinylated secondary antisera followed by streptavidin conjugated with Alexa fluor 488 or Alexa fluor 647 (3).

Immunostaining for bright-field microscopy and Giemsa staining were analyzed with an Olympus AX70 microscope (Olympus Optical, Hamburg, Germany). Immunofluorescence staining was documented as digitized false-color images obtained with an Olympus BX50WI laser scanning microscope (Olympus Optical, Hamburg, Germany).

Quantitation of RV-infected neurons, infiltrating leukocytes, and microglia in brain tissue. RV-infected neurons were quantified based on the number of RNP-immunopositive cells within the cerebral cortex and in the CA1-to-CA3 region of the hippocampal formation in at least three sections from each mouse

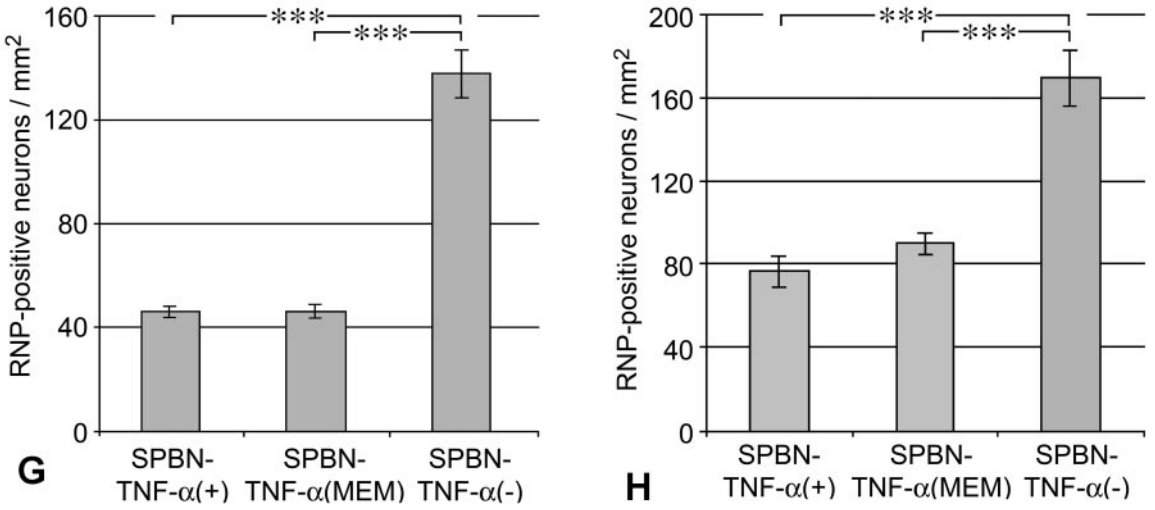

FIG. 6—*Continued.*

(n = 3 or 4) in the different experimental groups and calculated per mm^2. Giemsa-stained sections were used to quantify the number of leukocytes in the perivascular brain parenchyma and within the leptomeningeal space at the brain surface in at least three sections from each animal (n = 5) in the different experimental groups. Sections immunostained for CD3 were used to quantify T-cell numbers in the perivascular brain parenchyma and within the leptomeningeal space in at least three sections from each mouse (n = 3) in each group. Perivascular leukocyte and CD3-positive T-cell numbers were calculated per mm^2 perivascular area (s = 30). Leukocyte and CD3-positive T-cell numbers in the leptomeningeal space were calculated per mm length of leptomeninx (s = 12). Sections immunostained for Iba1 were used to quantify the proportional area of macrophages/microglial cells in the hippocampuses from the different experimental groups, using an MCID image analysis system (Imaging Research Inc., St. Catherines, Ontario, Canada). Data were expressed as mean values ± SEM. The significance of differences was calculated by ANOVA.

RESULTS

Expression of TNF-α by recombinant RVs. We engineered recombinant RVs that express either soluble TNF-α [SPBN-TNF-α(+)] or insoluble, membrane-bound TNF-α [SPBN-TNF-α(MEM)] (Fig. 1A) as an approach to determining whether noninvasive delivery of TNF-α affects the outcome of RV infection. To ensure that any observed effects were not due to the presence of a foreign nucleotide sequence in the RV rather than to TNF-α expression, we also engineered a recombinant virus expressing the TNF-α gene without ATG codons within the first 200 bases [SPBN-TNF-α(−)] (Fig. 1A).

The ability of the SPBN-TNF-α(+) construct to facilitate TNF-α secretion was demonstrated by ELISA, which revealed high levels of TNF-α in supernatants from SPBN-TNF-α(+)-infected BSR cells, but only low TNF-α levels in supernatants from SPBN-TNF-α(MEM)-infected cells and no detectable TNF-α secretion in the supernatants of SPBN-TNF-α(−)-infected BSR cells (Fig. 1B).

Confocal microscopy of SPBN-TNF-α(+)-infected NA cells revealed abundant TNF-α protein within the cytoplasm (Fig. 1C to L). SPBN-TNF-α(MEM)-infected NA cells, which released only low levels of TNF-α into the supernatant (data not shown), showed TNF-α-specific immunofluorescence staining on the membrane (Fig. 1F), indicating that TNF-α is produced in SPBN-TNF-α(MEM)-infected cells and is bound to the cell surface membrane. Consistent with the absence of TNF-α in the culture supernatants of SPBN-TNF-α(−)-infected BSR cells, NA cells did not express TNF-α protein (Fig. 1I).

Effect of recombinant-expressed TNF-α on RV replication in vitro. NA cells express both TNFR1 and TNFR2, as revealed by RT-PCR (data not shown), and were therefore used to examine the effect of recombinant-expressed TNF-α on virus replication. Single-step (low MOI) and especially multistep (high MOI) (Fig. 2A and B, respectively) growth curves for NA cells revealed replication rates for SPBN-TNF-α(+) and SPBN-TNF-α(MEM) that were significantly lower ($P <$ 0.001) than that for SPBN-TNF-α(−). On the other hand, treatment of SPBN-TNF-α(−)-infected NA cells with exogenous recombinant TNF-α (10 to 200 ng/ml) had no effect on virus production (data not shown), suggesting that the mechanism by which recombinant RV-expressed TNF-α exerts its antiviral effect is not triggered through interaction with the TNF-α receptors.

The lower replication rate for SPBN-TNF-α(+) could be due, at least in part, to an increase in cell death, since it is well known that TNF-α can induce apoptosis, mainly through engagement with TNFR1 (25). However, an analysis of the cell death rate of NA cells infected with SPBN-TNF-α(+) compared with that of SPBN-TNF-α(−)-infected NA cells revealed an increased mitochondrial membrane potential (Fig. 3A) and mitochondrial respiration (Fig. 3B) in SPBN-TNF-α(+)-infected NA cells, suggesting that decreased cell viability does not account for the decreased virus production observed for this construct.

TNF-α has been reported to trigger the production of IFN-α and IFN-β (26), which exhibit strong antiviral activity. However, NA cells treated with recombinant murine TNF-α showed no increased expression of IFN-α or IFN-β mRNA compared to untreated controls, and a bioassay did not reveal significant amounts of bioactive IFN-α/β in the supernatants of SPBN-TNF-α(+)- or SPBN-TNF-α(−)-infected NA cells (not shown). These data suggest that antiviral effects of TNF-α are not mediated by IFN-α or IFN-β.

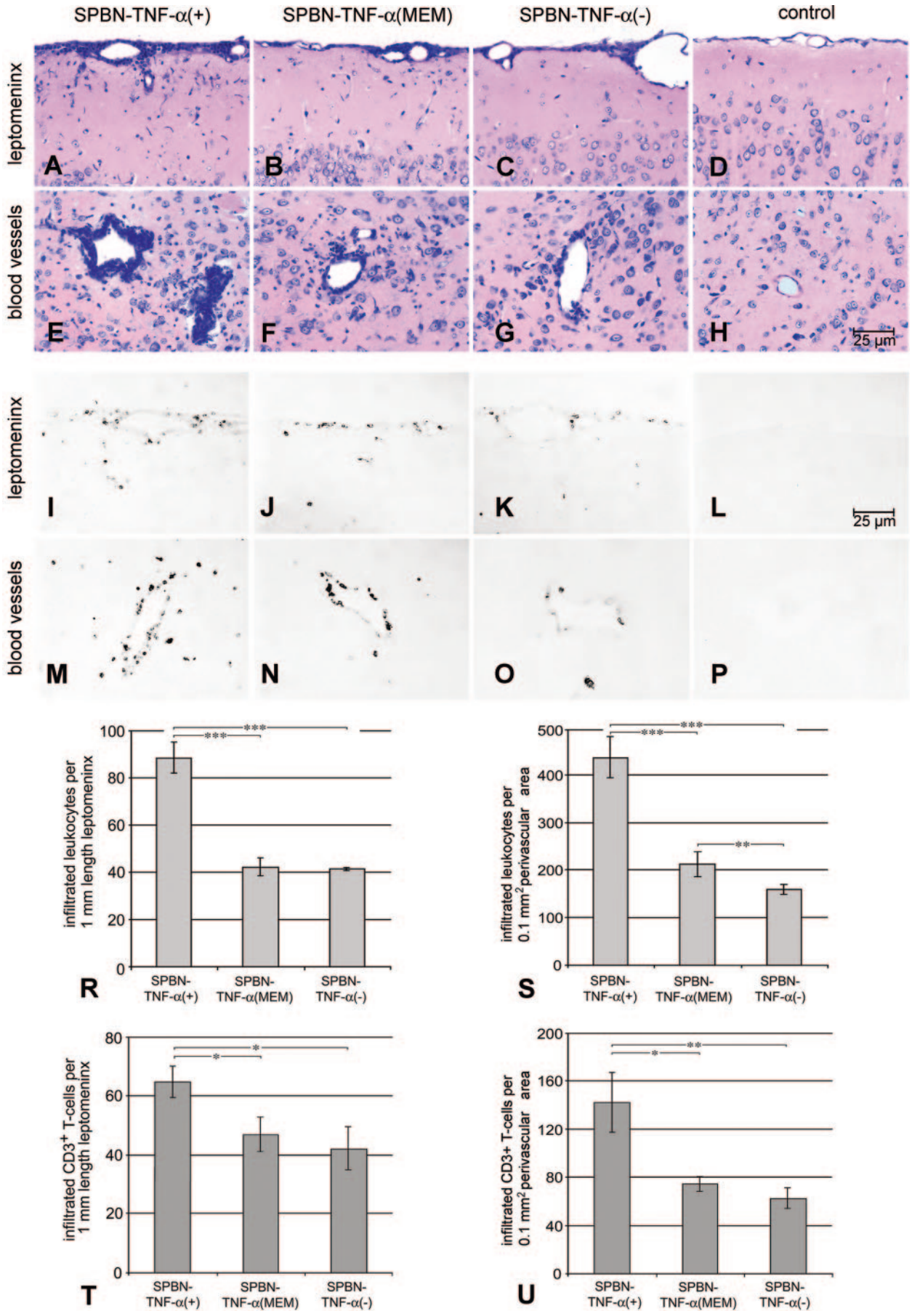
SPBN-TNF-α(+)
SPBN-TNF-α(MEM)
SPBN-TNF-α(-)
control
leptomeninx
blood vessels
A
B
C
D
E
F
G
H
25 µm
I
J
K
L
25 µm
M
N
O
P
infiltrated leukocytes per 1 mm length leptomeninx
R
infiltrated leukocytes per 0.1 mm² perivascular area
S
infiltrated CD3+ T-cells per 1 mm length leptomeninx
T
infiltrated CD3+ T-cells per 0.1 mm² perivascular area
U
SPBN-TNF-α(+)
SPBN-TNF-α(MEM)
SPBN-TNF-α(-)

Effects of recombinant RV-expressed TNF-α on survival of RV-infected mice. To determine whether the expression of TNF-α has an effect on the outcome of RV infection in vivo, adult female TNF-α KO mice were infected i.n. with 10^6 FFU SPBN-TNF-α(+), SPBN-TNF-α(MEM), or SPBN-TNF-α(−). TNF-α KO mice were used in order to exclude possible effects of endogenous TNF-α production by the host since RV infection induces TNF-α production in resident brain cells (24); the i.n. route was used to avoid any bias due to traumatic lesions of the brain associated with intracerebral injection. One hundred percent of mice infected with SPBN-TNF-α(+) survived the infection, and 20% of mice infected with SPBN-TNF-α(MEM) and 80% of mice infected with SPBN-TNF-α(−) died (Fig. 4A). On the other hand, TNF-α KO mice infected with SPBN-TNF-α(+) or SPBN-TNF-α(MEM) showed up to 20% and 12%, respectively, body weight loss over the duration of the experiment (Fig. 4B), as well as subtle neurological signs such as hyperactivity and increased irritability lasting almost the entire observation period. At 10 days p.i., SPBN-TNF-α(+)-infected TNF-α KO mice had markedly lower serum VNA titers (geometric mean VNA titer, 5.7) than did TNF-α KO mice infected with SPBN-TNF-α(−) (geometric mean VNA titer, 36.8) or SPBN-TNF-α(MEM) (geometric mean VNA titer, 22.0) (data not shown), suggesting that factors in addition to humoral immunity play a role in the TNF-α-mediated attenuation of RV infection.

Notably, the strong attenuating effect of recombinant RV-expressed TNF-α was also observed after i.n. infection of outbred Swiss Webster mice. Whereas none of the mice infected with SPBN-TNF-α(+) died, 90% of the mice infected with SPBN-TNF-α(−) succumbed to rabies encephalitis (data not shown).

Immunohistochemical analyses of virus load, leukocyte infiltration, and reactive microgliosis in brain tissue. Consistent with the expression of TNF-α in vitro, neurons infected in vivo with SPBN-TNF-α(+) or SPBN-TNF-α(MEM), but not neurons infected with SPBN-TNF-α(−), expressed TNF-α (Fig. 5). By 5 days after i.n. infection, only very small numbers of RNP-positive neurons were detected by immunohistological analysis of brains from TNF-α KO mice infected with the SPBN-TNF-α(+), SPBN-TNF-α(MEM), or SPBN-TNF-α(−) virus (data not shown). By day 10 p.i., infected neurons in SPBN-TNF-α(+)- and SPBN-TNF-α(MEM)-infected brains were significantly less prevalent in the cortex and hippocampus than those in SPBN-TNF-α(−)-infected brains (Fig. 6). An analysis of immune cell prevalence in brains infected with the different recombinant RVs revealed an inverse relationship between the number of virus-infected cells and the number of inflammatory leukocytes present in the leptomeningeal space and in perivascular areas of parenchymal blood vessels (Fig. 7). By 10 days p.i., the density of inflammatory leukocytes was highest in the leptomeninx and in perivascular areas of SPBN-TNF-α(+)-infected TNF-α KO mice (Fig. 7A and E), whereas lower densities of inflammatory leukocytes were detected in SPBN-TNF-α(MEM)- and SPBN-TNF-α(−)-infected brains (Fig. 7B, C, F, and G) and virtually no inflammatory leukocytes were seen in brains of noninfected mice (Fig. 7D and H). For perivascular areas, but not for the leptomeningeal space, the leukocyte density was significantly higher in SPBN-TNF-α(MEM)-infected brains than in SPBN-TNF-α(−)-infected brains (Fig. 7R and S).

Immunohistochemical analysis of T-cell infiltration in the brain parenchymas of mice infected with the different recombinant RVs revealed a significantly larger number of CD3-positive T cells in the brains of SPBN-TNF-α(+)-infected TNF-α KO mice than in SPBN-TNF-α(MEM)- or SPBN-TNF-α(−)-infected brains (Fig. 7I to P, T, and U). Note the absence of $CD3^+$ T cells in the leptomeninx and around blood vessels in noninfected control mouse brains (Fig. 7L and P).

To examine whether TNF-α has an effect on microglial activation, brain sections were stained immunocytochemically for the macrophage/microglial marker Iba1 and analyzed for changes in microglial morphology in accordance with an accepted classification (2). In noninfected control mice, microglial cells exhibited the typical phenotype of ramified microglia characterized by a small soma with thin, delicate projecting processes (Fig. 8A and B). The brains of all infected mice showed signs of microglial activation. However, while microglial cells of mice infected with SPBN-TNF-α(+) or SPBN-TNF-α(MEM) exhibited the characteristic phenotype of activated microglia, i.e., an enlarged, darkened soma and shorter, thicker, less branched processes (Fig. 8C to F), the morphology of microglial cells of SPBN-TNF-α(−)-infected mice was more amoeboid, with densely stained enlarged cell bodies and few short processes (Fig. 8G and H).

The activation of microglial cells was quantified based on the proportional area of Iba1-stained macrophages/microglial cells in the hippocampal regions of noninfected animals and in the three experimental groups. As shown in Fig. 8I, the proportion of the Iba1-positive macrophage/microglial area was significantly higher in the hippocampuses of mice infected with SPBN-TNF-α(+), SPBN-TNF-α(MEM), or SPBN-TNF-α(−) than in those of noninfected control mice. Moreover, reactive microgliosis was more pronounced, and the proportion of Iba1-positive macrophage/microglial areas was significantly higher, in mice infected with SPBN-TNF-α(+) or SPBN-TNF-α(MEM) than in mice infected with SPBN-TNF-α(−). Together, these data demonstrate that the extents of inflammatory reactions, reactive microgliosis, and T-cell infiltration

FIG. 7. Identification of cell infiltrates in recombinant RV-infected brains. The top and middle panels show Giemsa-stained brain sections (A to H) and CD3-immunostained brain sections (I to P) demonstrating leukocyte and T-cell infiltration, respectively, in the brains of TNF-α KO mice on day 10 after infection with SPBN-TNF-α(+), SPBN-TNF-α(MEM), or SPBN-TNF-α(−). Quantification of the numbers of infiltrated leukocytes (R and S) and $CD3^+$ T cells (T and U) within the leptomeninx of the brain surfaces (R and T) and in perivascular areas of parenchymal blood vessels (S and U) of TNF-α KO mice infected with SPBN-TNF-α(+), SPBN-TNF-α(MEM), or SPBN-TNF-α(−) is shown in the graphs. Data are expressed as mean values ± SEM; asterisks indicate significant differences (*, $P < 0.05$; **, $P < 0.01$; ***, $P < 0.001$) between the indicated experimental groups, as calculated by ANOVA.

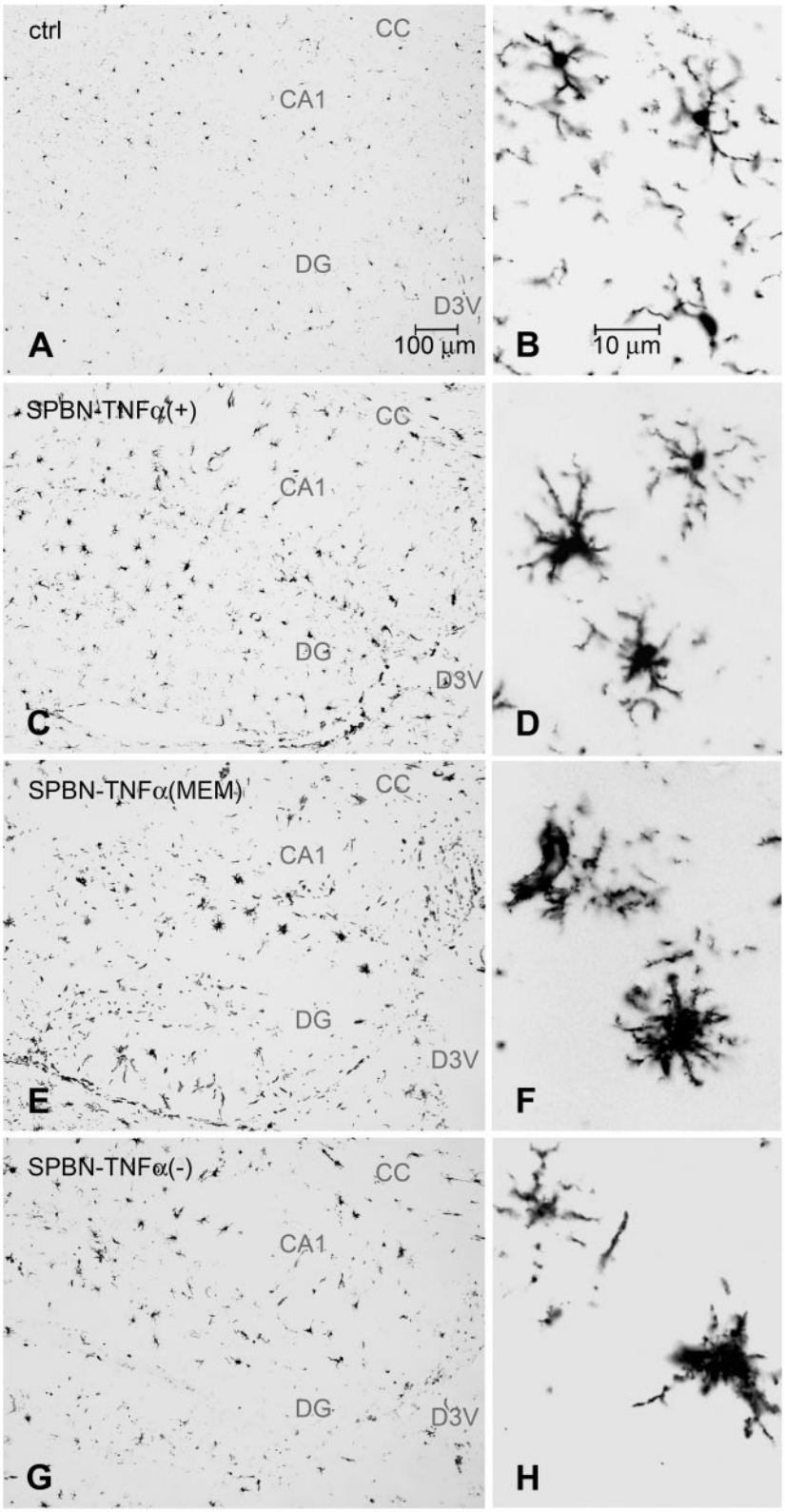

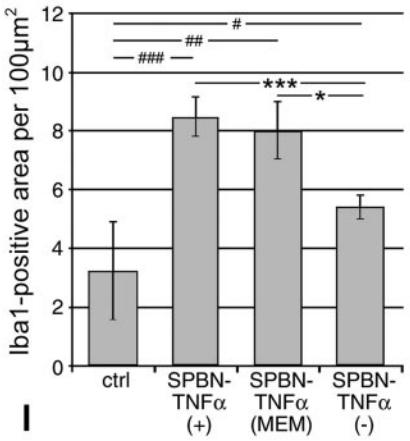

FIG. 8. (A to H) Immunohistochemical analysis of Iba1-positive microglial cells in the hippocampuses of TNF-α KO mice at 10 days p.i. Microglial cells in noninfected control animals (A and B) show the typical ramified phenotype of resting microglia. (E and F) Activated microglial cells in mice infected with SPBN-TNF-α(+) (C and D) and SPBN-TNF-α(MEM). (G and H) Activated microglial cells with a more ameboid morphology in SPBN-TNF-α(−)-infected brains. CA, CA region of hippocampus; CC, corpus callosum; D3V, dorsal third ventricle; DG, dentate gyrus. (I) Measurement of the areas of Iba1-positive microglial cells in the hippocampuses of noninfected control (ctrl) and RV-infected TNF-α KO mice on day 10 p.i. Data represent the means ± SEM of Iba1-immunopositive areas measured in 100 μm^2 of the hippocampal area. Three mice per group and six hippocampal tissue slices per mouse were used for the digital image analysis. Asterisks indicate significant differences (*, $P < 0.05$; **, $P < 0.01$; ***, $P < 0.001$) between the indicated experimental groups. #, significant differences (#, $P < 0.05$; ##, $P < 0.01$; ###, $P < 0.001$) between the noninfected control group and the indicated experimental groups, as calculated by ANOVA.

induced by TNF-α correlate inversely with the RV load in the brain and the lethality of the infection.

DISCUSSION

For this study, we used recombinant RVs expressing soluble or membrane-bound TNF-α to examine the effect of this proinflammatory cytokine on a neurotropic virus infection. TNF-α KO mice infected with the recombinant RV expressing soluble TNF-α [SPBN-TNF-α(+)] had significantly reduced virus loads in the brain and did not succumb to the infection compared to mice infected with recombinant RV containing an inactivated TNF-α gene [SPBN-TNF-α(−)], which showed significantly higher virus loads and a high mortality rate (80%). The reduced virus spread in brains infected with SPBN-TNF-α(+) was paralleled by enhanced CNS inflammation, including T-cell infiltration. Whereas the reduced virus load in brains infected with membrane-bound SPBN-TNF-α(MEM) was accompanied by only minimally increased inflammation, observed predominantly in perivascular areas, SPBN-TNF-α(+) and SPBN-TNF-α(MEM) induced similar degrees of microglial activation, to levels significantly higher than that produced by SPBN-TNF-α(−).

These findings suggest that TNF-α mediates its protective activity through different mechanisms, such as (i) direct inhibition of virus replication in neurons; (ii) accelerated clearance of RV infection via the induction of brain inflammatory processes, which open the blood brain barrier (BBB) to allow access of immune effectors such as RV-neutralizing antibodies and T cells to the infected neurons; and (iii) enhanced microglial activation, which likely contributes to the immune defense (19). It is probable that the outcome of RV infection is predominantly controlled by both leukocyte infiltration and microglial activation. Whereas 100% of mice survived infection with SPBN-TNF-α(+), which was associated with more extensive leukocyte infiltration than infection with SPBN-TNF-α(MEM), the degree of microglial activation by SPBN-TNF-α(MEM), though similar to that by SPBN-TNF-α(+), was apparently insufficient to confer complete protection. The finding that the pathogenicity of SPBN-TNF-α(−) for TNF-α knockouts was not significantly different from that for wild-type mice suggests that the induction of endogenous TNF-α in the brains of wild-type mice probably occurs too late to prevent a lethal outcome of the infection.

Our finding that TNF-α plays a protective and antiviral role in RV infection of the CNS is consistent with recent observations that indicate a neuroprotective role for TNF-α in various traumatic lesions and infections of the nervous system (12, 20, 30, 35). Our previous observation that the systemic administration of lipopolysaccharide leads to up-regulated TNFR1 expression in resident brain cells of the macrophage/microglial lineage, especially in those associated with blood vessels (3), supports the conclusion that TNF-α enhances the recruitment of infiltrating leukocytes, including T cells at the BBB. In fact, preliminary studies in our laboratory indicate that the endothelial activation marker P-selectin is induced in regions with enhanced leukocyte infiltration throughout the brains of mice infected with SPBN-TNF-α(+) and that TNFR2 mRNA-expressing inflammatory cells appear at the BBB after the injection of recombinant TNF-α (unpublished observations), raising the possibility that these cells are also stimulated by the recombinant RV-expressed TNF-α. There is evidence that CNS inflammatory processes contribute to the clearance of virus from the CNS (5, 22). Because the brain represents an immunoprivileged site, it is possible that TNF-α or members of the TNF superfamily abolish the immune privilege in particular sites of the brain, as shown for tumor sites (14, 39). Our data support such a role for TNF-α in the defense against infectious neurotropic pathogens such as rabies virus.

The mechanism by which TNF-α exerts its direct antiviral effect is not clear. The antiviral effect of recombinant RV-expressed TNF-α does not appear to be mediated through engagement with its specific membrane receptors, suggesting an intracellular function of TNF-α. There is increasing evidence that cytokines can exert biological effects as intracrine mediators within the cell (1, 40). Apoptosis or necrosis is unlikely to account for the antiviral effects of TNF-α since cell viability did not differ in NA cells infected with recombinant RVs expressing soluble, membrane-bound, or no TNF-α. IFN-α and IFN-β can also be excluded as potential antiviral effectors because no differences in IFN-α or IFN-β mRNA expression or IFN production were observed in NA cells infected with SPBN-TNF-α(+), SPBN-TNF-α(MEM), or SPBN-TNF-α(−).

In conclusion, our findings suggest that TNF-α exerts its protective activity in the brain directly through an as yet unknown antiviral mechanism and indirectly via the induction of inflammation.

ACKNOWLEDGMENTS

We thank Petra Lattermann and Marion Zibuschka for technical assistance.

This work was supported by Public Health Service grant AI45097-6, the Deutsche Forschungsgemeinschaft SFB 297, Schwerpunkt Mikroglia, and the Volkswagen-Stiftung.

REFERENCES

1. **Alberti, L., M. C. Thomachot, T. Bachelot, C. Menetrier-Caux, I. Puisieux, and J. Y. Blay.** 2004. IL-6 as an intracrine growth factor for renal carcinoma cell lines. Int. J. Cancer **111:**653–661.
2. **Ayoub, A. E., and A. K. Salm.** 2003. Increased morphological diversity of microglia in the activated hypothalamic supraoptic nucleus. J. Neurosci. **23:**7759–7766.
3. **Bette, M., O. Kaut, M. K. Schafer, and E. Weihe.** 2003. Constitutive expression of p55TNFR mRNA and mitogen-specific up-regulation of TNF alpha and p75TNFR mRNA in mouse brain. J. Comp. Neurol. **465:**417–430.
4. **Bette, M., M. K.-H. Schäfer, N. van Rooijen, E. Weihe, and B. Fleischer.** 1993. Distribution and kinetics of superantigen-induced cytokine gene expression in mouse spleen. J. Exp. Med. **178:**1531–1539.
5. **Biermer, M., R. Puro, and R. J. Schneider.** 2003. Tumor necrosis factor alpha inhibition of hepatitis B virus replication involves disruption of capsid integrity through activation of NF-kappaB. J. Virol. **77:**4033–4042.
6. **Blum, A., and H. Miller.** 2000. The major histocompatibility complex and inflammation. South Med. J. **93:**169–172.
7. **Camelo, S., J. Castellanos, M. Lafage, and M. Lafon.** 2001. Rabies virus ocular disease: T-cell-dependent protection is under the control of signaling by the p55 tumor necrosis factor alpha receptor, p55TNFR. J. Virol. **75:** 3427–3434.
8. **Camelo, S., M. Lafage, A. Galelli, and M. Lafon.** 2001. Selective role for the p55 Kd TNF-alpha receptor in immune unresponsiveness induced by an acute viral encephalitis. J. Neuroimmunol. **113:**95–108.
9. **Cox, J. H., B. Dietzschold, and L. G. Schneider.** 1977. Rabies virus glycoprotein. II. Biological and serological characterization. Infect. Immun. **16:** 754–759.
10. **Decoster, E., B. Vanhaesebroeck, P. Vandenabeele, J. Grooten, and W. Fiers.** 1995. Generation and biological characterization of membrane-bound, uncleavable murine tumor necrosis factor. J. Biol. Chem. **270:**18473–18478.
11. **Depboylu, C., T. A. Reinhart, O. Takikawa, Y. Imai, H. Maeda, H. Mitsuya, D. Rausch, L. E. Eiden, and E. Weihe.** 2004. Brain virus burden and in-

doleamine-2,3-dioxygenase expression during lentiviral infection of rhesus monkey are concomitantly lowered by 6-chloro-2′,3′-dideoxyguanosine. Eur. J. Neurosci. **19:**2997–3005.
12. **Diem, R., R. Meyer, J. H. Weishaupt, and M. Bahr.** 2001. Reduction of potassium currents and phosphatidylinositol 3-kinase-dependent AKT phosphorylation by tumor necrosis factor-(alpha) rescues axotomized retinal ganglion cells from retrograde cell death in vivo. J. Neurosci. **21:**2058–2066.
13. **Dietzschold, B., M. Kao, Y. M. Zheng, Z. Y. Chen, G. Maul, Z. F. Fu, C. E. Rupprecht, and H. Koprowski.** 1992. Delineation of putative mechanisms involved in antibody-mediated clearance of rabies virus from the central nervous system. Proc. Natl. Acad. Sci. USA **89:**7252–7256.
14. **Homey, B., A. Muller, and A. Zlotnik.** 2002. Chemokines: agents for the immunotherapy of cancer? Nat. Rev. Immunol. **2:**175–184.
15. **Hooper, D. C., K. Morimoto, M. Bette, E. Weihe, H. Koprowski, and B. Dietzschold.** 1998. Collaboration of antibody and inflammation in clearance of rabies virus from the central nervous system. J. Virol. **72:**3711–3719.
16. **Jacobsen, H., J. Mestan, S. Mittnacht, and C. W. Dieffenbach.** 1989. Beta interferon subtype 1 induction by tumor necrosis factor. Mol. Cell. Biol. **9:**3037–3042.
17. **Li, Y., A. Ji, E. Weihe, and M. K. Schafer.** 2004. Cell-specific expression and lipopolysaccharide-induced regulation of tumor necrosis factor alpha (TNF-alpha) and TNF receptors in rat dorsal root ganglion. J. Neurosci. **24:**9623–9631.
18. **Locksley, R. M., N. Killeen, and M. J. Lenardo.** 2001. The TNF and TNF receptor superfamilies: integrating mammalian biology. Cell **104:**487–501.
19. **Lokensgard, J. R., S. Hu, W. Sheng, M. vanOijen, D. Cox, M. C. Cheeran, and P. K. Peterson.** 2001. Robust expression of TNF-alpha, IL-1beta, RANTES, and IP-10 by human microglial cells during nonproductive infection with herpes simplex virus. J. Neurovirol. **7:**208–219.
20. **Marchetti, L., M. Klein, K. Schlett, K. Pfizenmaier, and U. L. Eisel.** 2004. Tumor necrosis factor (TNF)-mediated neuroprotection against glutamate-induced excitotoxicity is enhanced by *N*-methyl-D-aspartate receptor activation. Essential role of a TNF receptor 2-mediated phosphatidylinositol 3-kinase-dependent NF-kappa B pathway. J. Biol. Chem. **279:**32869–32881.
21. **Mestan, J., W. Digel, S. Mittnacht, H. Hillen, D. Blohm, A. Moller, H. Jacobsen, and H. Kirchner.** 1986. Antiviral effects of recombinant tumour necrosis factor in vitro. Nature **323:**816–819.
22. **Morimoto, K., J. P. McGettigan, H. D. Foley, D. C. Hooper, B. Dietzschold, and M. J. Schnell.** 2001. Genetic engineering of live rabies vaccines. Vaccine **19:**3543–3551.
23. **Morimoto, K., M. Patel, S. Corisdeo, D. C. Hooper, Z. F. Fu, C. E. Rupprecht, H. Koprowski, and B. Dietzschold.** 1996. Characterization of a unique variant of bat rabies virus responsible for newly emerging human cases in North America. Proc. Natl. Acad. Sci. USA **93:**5653–5658.
24. **Nuovo, G. J., D. L. Defaria, J. G. Chanona-Vilchi, and Y. Zhang.** 2005. Molecular detection of rabies encephalitis and correlation with cytokine expression. Mod. Pathol. **18:**62–67.
25. **Paleolog, E. M., S. A. Delasalle, W. A. Buurman, and M. Feldmann.** 1994. Functional activities of receptors for tumor necrosis factor-alpha on human vascular endothelial cells. Blood **84:**2578–2590.
26. **Pestka, S., C. D. Krause, and M. R. Walter.** 2004. Interferons, interferon-like cytokines, and their receptors. Immunol. Rev. **202:**8–32.
27. **Peterson, K. E., S. Hughes, D. E. Dimcheff, K. Wehrly, and B. Chesebro.** 2004. Separate sequences in a murine retroviral envelope protein mediate neuropathogenesis by complementary mechanisms with differing requirements for tumor necrosis factor alpha. J. Virol. **78:**13104–13112.
28. **Pulmanausahakul, R., M. Faber, K. Morimoto, S. Spitsin, E. Weihe, D. C. Hooper, M. J. Schnell, and B. Dietzschold.** 2001. Overexpression of cytochrome *c* by a recombinant rabies virus attenuates pathogenicity and enhances antiviral immunity. J. Virol. **75:**10800–10807.
29. **Ruby, J., H. Bluethmann, and J. J. Peschon.** 1997. Antiviral activity of tumor necrosis factor (TNF) is mediated via p55 and p75 TNF receptors. J. Exp. Med. **186:**1591–1596.
30. **Saha, R. N., and K. Pahan.** 2003. Tumor necrosis factor-alpha at the crossroads of neuronal life and death during HIV-associated dementia. J. Neurochem. **86:**1057–1071.
31. **Schnell, M. J., T. Mebatsion, and K. K. Conzelmann.** 1994. Infectious rabies viruses from cloned cDNA. EMBO J. **13:**4195–4203.
32. **Seo, S. H., and R. G. Webster.** 2002. Tumor necrosis factor alpha exerts powerful anti-influenza virus effects in lung epithelial cells. J. Virol. **76:**1071–1076.
33. **Smith, R. A., and C. Baglioni.** 1987. The active form of tumor necrosis factor is a trimer. J. Biol. Chem. **262:**6951–6954.
34. **Sriram, S., D. J. Topham, L. Carroll, M. Shenoy, A. Adesina, and J. E. Craighead.** 1991. In vivo administration of TNF-alpha prevents EMC-M virus induced viral encephalitis. Int. Immunol. **3:**641–645.
35. **Stoll, G., S. Jander, and M. Schroeter.** 2000. Cytokines in CNS disorders: neurotoxicity versus neuroprotection. J. Neural Transm. **59**(Suppl.)**:**81–89.
36. **Tracey, K. J., and A. Cerami.** 1994. Tumor necrosis factor: a pleiotropic cytokine and therapeutic target. Annu. Rev. Med. **45:**491–503.
37. **Vistica, D. T., P. Skehan, D. Scudiero, A. Monks, A. Pittman, and M. R. Boyd.** 1991. Tetrazolium-based assays for cellular viability: a critical examination of selected parameters affecting formazan production. Cancer Res. **51:**2515–2520.
38. **Wajant, H., K. Pfizenmaier, and P. Scheurich.** 2003. Tumor necrosis factor signaling. Cell Death Differ. **10:**45–65.
39. **Wang, J., V. C. Asensio, and I. L. Campbell.** 2002. Cytokines and chemokines as mediators of protection and injury in the central nervous system assessed in transgenic mice. Curr. Top. Microbiol. Immunol. **265:**23–48.
40. **Werman, A., R. Werman-Venkert, R. White, J. K. Lee, B. Werman, Y. Krelin, E. Voronov, C. A. Dinarello, and R. N. Apte.** 2004. The precursor form of IL-1alpha is an intracrine proinflammatory activator of transcription. Proc. Natl. Acad. Sci. USA **101:**2434–2439.
41. **Wiktor, T. J., R. I. Macfarlan, C. M. Foggin, and H. Koprowski.** 1984. Antigenic analysis of rabies and Mokola virus from Zimbabwe using monoclonal antibodies. Dev. Biol. Stand. **57:**199–211.